infrastructures

MDPI

Article

Enhancing Moisture Damage Resistance in Asphalt Concrete: The Role of Mix Variables, Hydrated Lime and Nanomaterials

Noor N. Adwar and Amjad H. Albayati *

Department of Civil Engineering, University of Baghdad, Baghdad 17001, Iraq; noor.adwar2201m@coeng.uobaghdad.edu.iq
* Correspondence: a.khalil@uobaghdad.edu.iq

Abstract: Moisture-induced damage is a serious problem that severely impairs asphaltic pavement and affects road serviceability. This study examined numerous variables in asphalt concrete mixtures to assess their impact on moisture damage resistance. Mix design parameters such as the asphalt content (AC) and aggregate passing sieve No. 4 (PNo. 4) were considered as variables during this study. Additionally, hydrated lime (HL) was utilized as a partial substitute for limestone dust (LS) filler at 1.5% by weight of the aggregate in asphalt concrete mixtures for the surface layer. This study also investigated the potential enhancement of traditional asphalt binders and mixtures by adding nano-additives, specifically nano-silica oxide (NS) and nano-titanium dioxide (NT), at rates ranging from 0% to 6% by weight of the asphalt binder. To quantify the moisture damage resistance of the asphalt concrete mixes, two types of laboratory tests were employed: the tensile strength ratio (TSR) and the index of retained strength (IRS). The former characterizes moisture damage using tensile strength, whereas the latter uses compression strength. The physical properties of the asphalt binder, such as its penetration, softening point, and ductility, were also evaluated to identify the effects of the nanomaterials. The results indicated that variations in the mix design variables significantly affected the moisture damage resistance of the asphalt concrete mixtures. The maximum improvement values were obtained at the optimum asphalt content (OAC) and PNo. 4 (mid-range + 6%) with TSR values of 80.45 and 82.46 and IRS values of 74.39 and 77.14, respectively. Modifying asphalt concrete mixtures with 1.5% HL resulted in improved moisture resistance compared with mixtures without HL (0% HL) at each PNo. 4 level, reaching superior performance at PNo. 4 (mid-range + 6%) by 4.58% and 3.96% in the TSR and IRS tests, respectively. Additionally, both NS and NT enhanced the physical properties of the asphalt binder, leading to substantial enhancements in asphalt concrete mixture performance against moisture damage. A 6% dosage of NS and NT showed the best performance, with NS performing slightly better than NT. TSR was increased by 14.72 and 11.55 and IRS by 15.60 and 12.75, respectively, with 6% NS and NT compared with mixtures without nanomaterials (0% NM).

Keywords: moisture damage; nano-silica; nano-titanium; asphalt concrete; tensile strength ratio; index of retained strength

Citation: Adwar, N.N.; Albayati, A.H. Enhancing Moisture Damage Resistance in Asphalt Concrete: The Role of Mix Variables, Hydrated Lime and Nanomaterials. *Infrastructures* **2024**, *9*, 173. https://doi.org/10.3390/infrastructures9100173

Academic Editors: Chris Goodier and Hugo Silva

Received: 6 August 2024
Revised: 6 September 2024
Accepted: 26 September 2024
Published: 1 October 2024

1. Introduction

The challenge for the road pavement construction sector is to design and construct superior-performing asphalt materials to satisfy the growing demand for increased axle loadings and fluctuations in climate conditions that contribute to pavement distress such as moisture damage, fatigue cracking, and rutting [1]. These kinds of distress impair the lifespan and performance of flexible pavements [2]. Moisture-induced damage to the asphalt concrete surface course is a principal reason for premature pavement failure [3]. Therefore, it is essential to understand the mechanism of moisture damage and to find an appropriate mix of aggregate and asphalt cement to address this issue. Moisture damage can typically be categorized into two main mechanisms: (a) loss of adhesion and (b) loss of cohesion. Loss of adhesion occurs when water seeps between the aggregate and the

asphalt, stripping away the asphalt film. Loss of cohesion happens when the asphalt concrete mastic softens. These mechanisms are interconnected, so a pavement affected by moisture damage may display these effects in combination [4–11]. Several studies have indicated that the driving load leads to a negative-pressure pumping action that continuously scours the interface between the asphalt and aggregate, accelerating the stripping of the asphalt layer from the aggregate surface. Further expansion of interior microcracks and weak contact surfaces in asphalt concrete mixtures contributes to the degradation of their physical and mechanical properties, leading to water damage and other road surface problems. Therefore, cohesive failure at the asphalt–asphalt interface and adhesion failure at the asphalt–aggregate interface are likely to occur [12–16].

Many variables affect moisture damage in asphalt pavements. Some of these variables are related to the asphalt mix design and the quality of the materials that form the asphalt concrete mixtures, such as aggregates and asphalt cement [17]. The physical and chemical characteristics of these components seriously impact asphalt concrete efficiency in resisting moisture damage [18–20]. Several studies have been conducted to investigate the ability of mix design variables to mitigate the effects of moisture damage. These studies are outlined in Table 1.

Table 1. A review of using mix variables for asphalt mixes.

Variables	Description	Results	References
Asphalt content	AC: 4.3%, 4.8%, and 5.3%	The mixes with OAC performed better at withstanding moisture damage under the compressive strength test and double-punch shear test.	[21]
	OAC and OAC ± 0.5%	Increased AC above the optimum level reduced the friction (interlocking) between aggregate particles, resulting in a drawback in asphalt concrete mixture performance.	[22]
	Two-level content (4.2% and 5.2%)	A lower AC proved to be more effective in withstanding asphalt mixture distress.	[23]
	OAC and OAC ± 0.6%	The findings indicated that the mixes formed with OAC and OAC + 0.6% meet the required moisture damage resistance (TSR $\geq$ 80%).	[24]
Aggregate gradation	Two aggregate types (slag and granite) with fine and coarse gradations	Mixtures with a finer gradation tended to be less susceptible to moisture damage than mixes with a coarser gradation.	[25]
	Dense bituminous macadam and bituminous concrete were utilized with three different gradations (finer, coarser, and normal) for each mix.	The mixes with fine gradations (upper limit) were better than the mixes with medium or lower gradations regarding Marshall properties, tensile strength ratio, and permanent deformation for both types of mixes.	[26]
	Lower limit, mid-range, and upper limit gradations were attempted.	Lower gradations demonstrated better performance in terms of moisture damage and permanent deformation.	[27]
	A coarse mix and a fine mix of aggregates were chosen to create the overall structure.	This study inferred that finer-gradation blends exhibit greater resistance to moisture damage in comparison with coarser-gradation combinations.	[28]

Table 1. *Cont.*

Variables	Description	Results	References
HL addition by weight of the filler	HL	The results indicated significant improvements in aggregate bonding and mixture strength.	[29,30]
	HL	The addition of 2.5% HL can significantly improve asphalt mixtures' resistance to water, freezing, and thawing cracks.	[31]
	HL	HL can interact with asphalt functional groups to create a waterproofing compound that effectively reduces moisture in mixtures.	[32]
	HL	Three different sizes of HL were used: micro-, sub-nano-, and nanoscale. This investigation showed a significant correlation between the size of the HL particles and the asphalt mixtures' ability to mitigate distress.	[33]
	HL and cement kiln dust	The mixes containing HL and cement kiln dust had a higher tensile strength ratio than those with no additions.	[34]
	Cement, brake pad powder, LS, and HL	HL performed better on pavements in terms of withstanding moisture damage.	[35]

Flexible pavement failures can be effectively controlled with proper construction techniques and materials that outperform conventional materials [36]. One of the most effective techniques for improving asphalt concrete's performance properties is employing different additive materials, such as polymers, fibers, and nanomaterials (NMs) [37–40]. Modifiers generally enhance the mixture's properties, reducing moisture damage, fatigue, low-temperature cracks, permanent deformation, and aging resistance, thereby improving the overall performance of the mixture [41–44].

Nanotechnology is a highly adaptable and inventive technology in the material industry, with applications in a wide range of fields [45,46]. Nanomaterial manufacturing reduces the dimensions from normal to nano-size, altering the surface structures, surface energies, and physicochemical characteristics of the original materials. A nanoparticle is marked by at least one dimension that is smaller than 100 nm [40,47,48]. Reducing a material to the nanoscale significantly increases the surface-area-to-volume ratio, which enhances the surface energy of the particles. This increased surface energy arises because a larger proportion of atoms is exposed on the surface compared with bulkier materials, leading to higher reactivity and stronger interactions with surrounding materials. As a result, nanoparticles exhibit improved bonding capabilities with asphalt binders, making them effective in mitigating various asphalt concrete distresses, including moisture damage [47,48]. Owing to their distinctive properties such as high surface area, durability, dispersion ability, and chemical purity, nanomaterials have been studied extensively for their potential to enhance asphalt performance. These studies are outlined in Table 2.

Table 2. A review of research using NS and NT for asphalt concrete mixes.

NM	NM Percent (% by Weight of Asphalt)	Results	References
NS	0, 2, 4, 6	The optimal dosage for enhancing the mixture's performance was 4% NS, and the results indicated that NS considerably reduces sensitivity to oxidative aging.	[45]
NS	0, 2, 4, 6	The viscosity of the modified bitumen with 6% NS was significantly increased compared with that of the neat asphalt. Additionally, storage stability improved at the same percent, which preserved the binder stability at high temperatures.	[49]
NT	0, 3, 6	NT strengthened the adhesion between the aggregate and asphalt. Moreover, the asphalt pavement distress was reduced.	[50]

Table 2. *Cont.*

NM	NM Percent (% by Weight of Asphalt)	Results	References
NS	0, 0.1, 0.3, 0.5	SEM images revealed a uniform distribution of the NS throughout the asphalt matrix. The 0.3% NS dosage had better moisture damage resistance, with an increment of 26.25% compared with the non-NS asphalt mixture.	[51]
NT	0, 2, 4, 6, 8, 10	The bitumen's consistency properties (penetration and softening point) were greatly enhanced. NT increased the modified asphalt binder stiffness. Samples including NT increased the mixture's resistance to water.	[52]
NS	0, 0.2, 0.4, 0.7, 0.9	Indirect tensile strength and compressive strength were greatly improved when employing NS as an anti-stripping agent.	[53]
NS	0, 0.2, 0.4, 0.7, 0.9	Incorporating NS increased the asphalt mixture's resistance to moisture sensitivity at various air void contents (4%, 5%, and 6%).	[54]
NT	3, 6, 9, 12, 15	The asphalt binder's mechanical and rheological characteristics were improved by adding the photocatalytic semiconductor nano-TiO_2.	[55]
NT	0, 1, 2, 3, 4, 5	The stone–mastic asphalt's mechanical characteristics were improved by incorporating 3% NT. There was a 3% to 5% NT optimum value in enhancing the consistency properties of bitumen (penetration and softening point).	[56]
NT	0, 1, 3, 5, 7	Viscosity was increased and bituminous sensitivity was decreased with the inclusion of NT. Adding 5% NT improved the physical characteristics of the asphalt and its resistance to fatigue cracking and rutting.	[57]

The literature review reveals a significant gap in understanding the combined effects of mix design variables and modifiers on moisture damage resistance in asphalt concrete mixtures. Previous studies have not fully explored how parameters such as asphalt content (AC) and aggregate gradation (PNo. 4) along with additives like hydrated lime (HL), nano-silica oxide (NS), and nano-titanium dioxide (NT) interact to influence moisture damage resistance. This research addresses this gap by systematically evaluating the effect of these factors on the moisture damage resistance of the mixtures. Moisture damage was determined by utilizing two types of tests: the tensile strength ratio and the index of retained compressive strength. This study also investigated the effect of NS and NT on the physical properties of traditional asphalt binder, including penetration, softening point, and ductility, providing valuable insight into possible enhancements of asphalt concrete mixtures using these nanomaterials, hydrated lime, and mix design variables, allowing the design and construction of more durable and longer-lasting asphalt pavements.

2. Materials

2.1. Asphalt Cement

Asphalt cement (40–50) of penetration grade was utilized, which is a common type for paving roads in Iraq. It was acquired from Baghdad's Al-Daurah refinery. Table 3 displays the asphalt cement's physical properties, which are within the specification limits set by the State Commission of Roads and Bridges [58].

Table 3. Physical properties of asphalt.

Test	Units	ASTM Designation	Result	SCRB Specification
Penetration	1/10 mm	D5	44	40–50
Ductility	cm	D113	138	≥100
Softening point (ring and ball)	°C	D36	52	-----
Kinematics viscosity, at 135 °C	Pa.s	D2170	450	≥400
Flash point (Cleveland open cup)	°C	D92	249	≥232
Specific gravity	-----	D70	1.03	-----
Residue from thin-film oven test.				
Retained penetration of original (%)	1/10 mm	D5	63	>55
Ductility	cm	D113	76	>25

2.2. Aggregate

The aggregate was crushed quartz obtained from the AI-Nibaie quarry, located northeast of Baghdad. The coarse and fine aggregates were sieved and recombined following the mid-range gradation for the Type IIIA mix with a nominal maximum size of 12.5 mm, which is used for wearing course pavement as per SCRB specifications [58]. Figure 1 displays the aggregate gradation curve. Additionally, two other gradations were considered as mix design variables in this work based on the tolerances recommended by SCRB specifications: the first represents a fine gradation, including mid-range passing sieve No. 4 plus 6%, and the second represents a coarse gradation, including mid-range passing sieve No. 4 minus 6%. The findings of the routine testing to assess the aggregates' physical characteristics are displayed in Table 4.

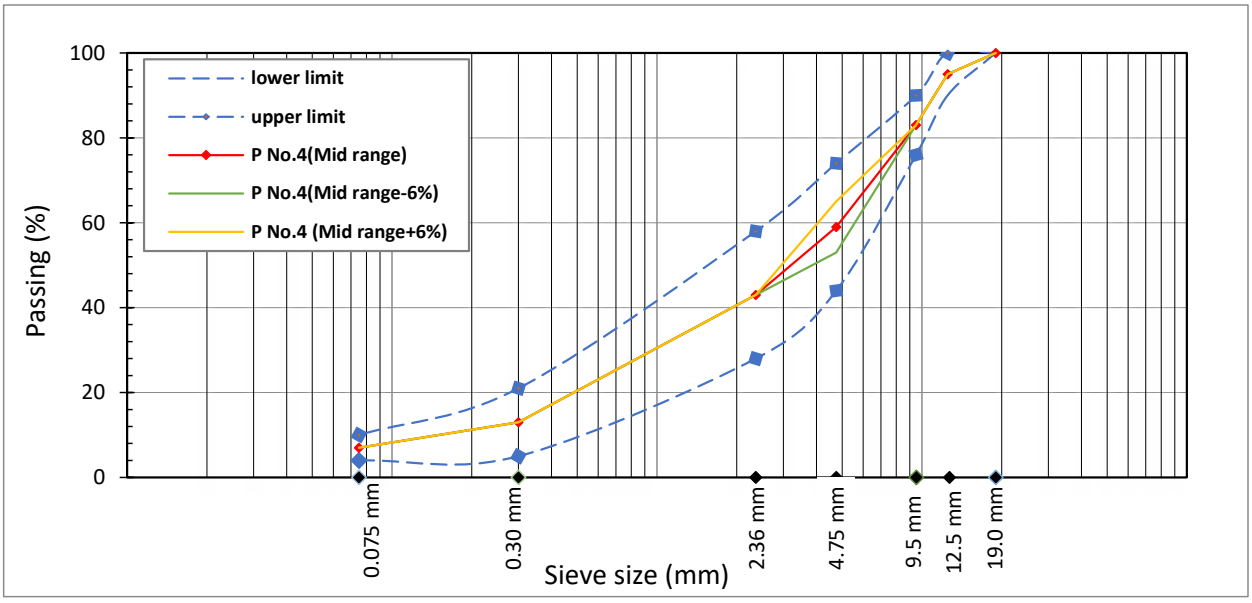

Figure 1. Design aggregate gradation.

Table 4. Physical properties of aggregates.

Test	ASTM Specification	Result	SCRB Specification
Coarse aggregate			
Bulk specific gravity	C127	2.610	-----
Apparent specific gravity	C127	2.642	-----
Water absorption	C127	0.54	-----
Los Angeles abrasion %	C131	16. 6	30 max
Fine aggregate			
Bulk specific gravity	C128	2.651	------
Apparent specific gravity	C128	2.684	------
Water absorption	C128	0.723	-------

2.3. Mineral Filler

Limestone dust (LS) was utilized as the primary filler type, representing 7% of the total aggregate weight, which is the mid-range specified by the SCRB [58]. Additionally, hydrated lime (HL) was used as a substitute for LS at a rate of 1.5% by weight of the aggregate, based on recommendations stated in SCRB to enhance moisture damage resistance. The physical characteristics of HL and LS, obtained from the Karbala governorate's lime factory, are shown in Table 5.

Table 5. Physical properties of LS and HL.

Material Property	Limestone Dust	Hydrated Lime
Specific gravity	2.72	2.42
Passing No.200 (%)	93	98
Surface area (m^2/gm)	244	398

Scanning electron microscopy (SEM) images at 1000× magnification, as displayed in Figure 2, visually compare the crystalline structure and the surface morphology of LS and HL. LS has an irregular shape with a smooth surface. In contrast, HL particles appear granular, with a rough surface texture. The roughness of the HL particles increases the surface area, which can improve the mechanical interlocking within the asphalt mixture. This enhanced interlocking ability contributes to the increased cohesion and stability of the asphalt concrete, potentially leading to improved resistance against moisture damage.

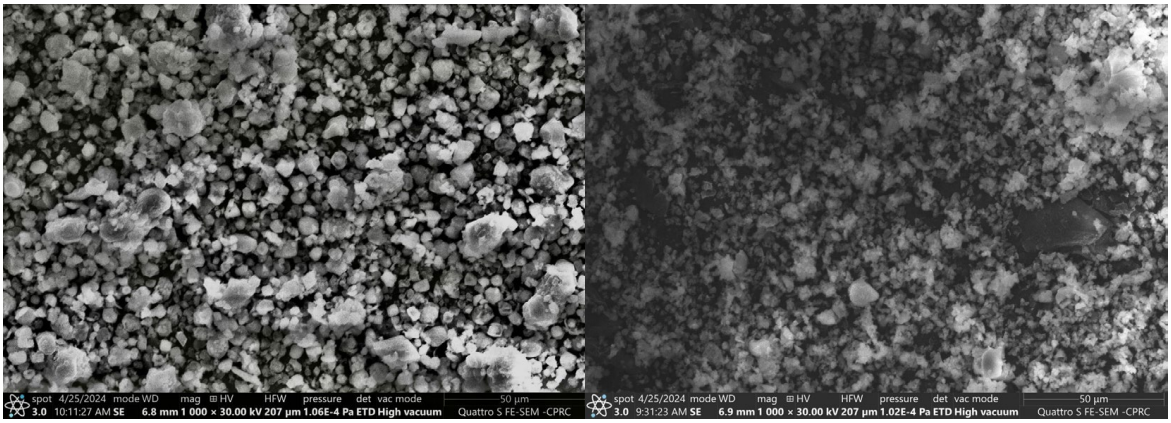

(**a**) (**b**)

Figure 2. SEM of (**a**) LS and (**b**) HL.

2.4. Nanomaterials Additives

The nanomaterials NS and NT were used in this study owing to their distinct properties in enhancing the asphalt mixture's performance. NS usually has a significant surface area and better dispersion abilities, while NT has high purity and very low opacity. Table 6 illustrates the physical properties of these nanomaterials.

Table 6. Nanomaterial physical properties.

Properties	Nanomaterials	
	NS	**NT**
Chemical formula	SiO_2	TiO_2
Appearance	White powder	White powder
Average particle size, nm	25~60	20~55
Specific surface area, m^2/gm	190~250	120~160
Purity, %	99.8	99.9
Meting point, °C	2030	1730
Bulk density, g/mL	0.08	0.51
Molecule wt., g/mol	60.08	85.42

The SEM images at 120 kx magnification, as displayed in Figure 3, were employed to examine the crystalline structure and surface morphology of the nanomaterials used in this study. The SEM image of NS shows agglomerated spherical particles that are highly dense and rather homogeneous, with a large surface area. Depending on their structure, NS particles may possess an enormous contact surface, which stiffens the binder. On the other hand, the SEM image of NT reveals that uniform spherical particles typically appear in cluster form. The surface structure of NT provides an even surface area, making it easier to mix with asphalt binder, which can result in a homogeneous dispersion in the mixture.

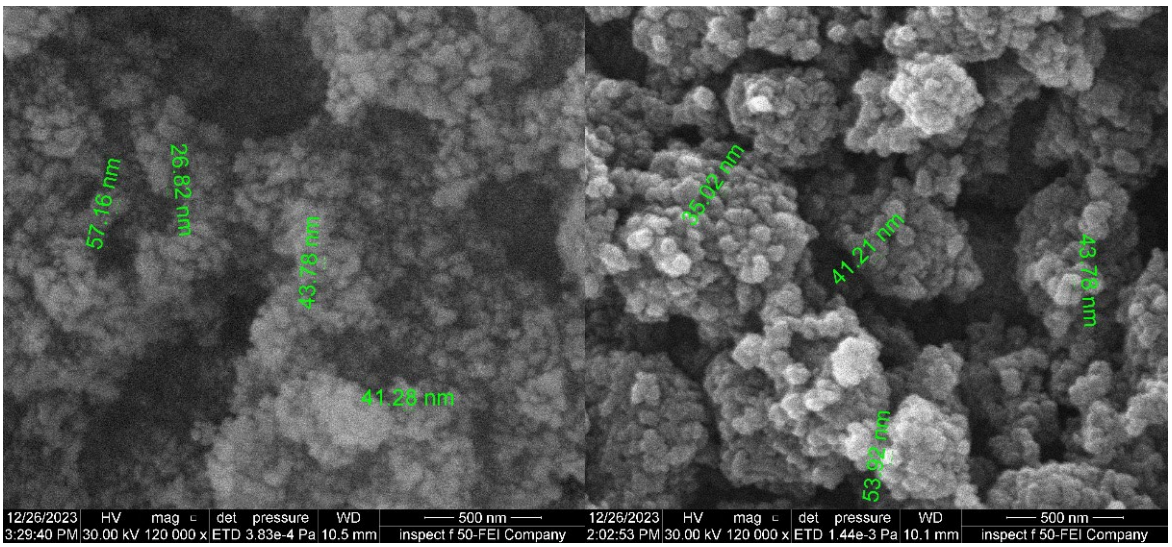

(**a**) (**b**)

Figure 3. SEM of (**a**) NS and (**b**) NT.

Energy-dispersive X-ray (EDX) spectra of the nanomaterials were also obtained, as shown in Figures 4 and 5. Tables 7 and 8 provide a summary of the elemental compositions of each material. EDX spectra were obtained from specific regions on the surface of the nanoparticle material to determine the nanomaterial composition and surface atom

distribution. As demonstrated in Figure 4, SiO_2 showed high-intensity peaks of silicon (Si) and oxygen (O), illustrating the nature of pure SiO_2 nanoparticles. According to the EDX analysis, the elemental percentages of Si and O were 42.7% and 56.6%, respectively. The EDX analysis of TiO_2 nanoparticles detected Ti, O, S, Si, Mg, Ca, and V elements, as shown in Figure 5. According to the results, the weight percentages of Ti and O were comparatively higher than those of the other elements because of the structure of their nanoparticles, with percentages of 39.4% and 57.1%, respectively.

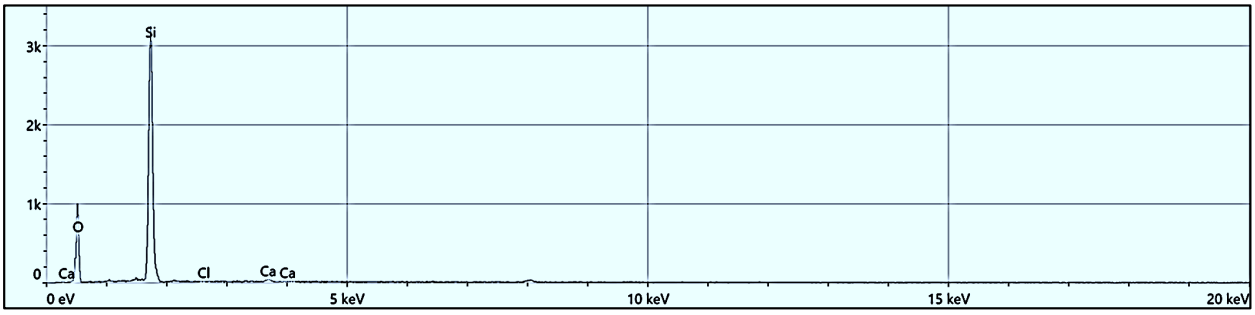

Figure 4. EDX spectrum of nano-SiO_2.

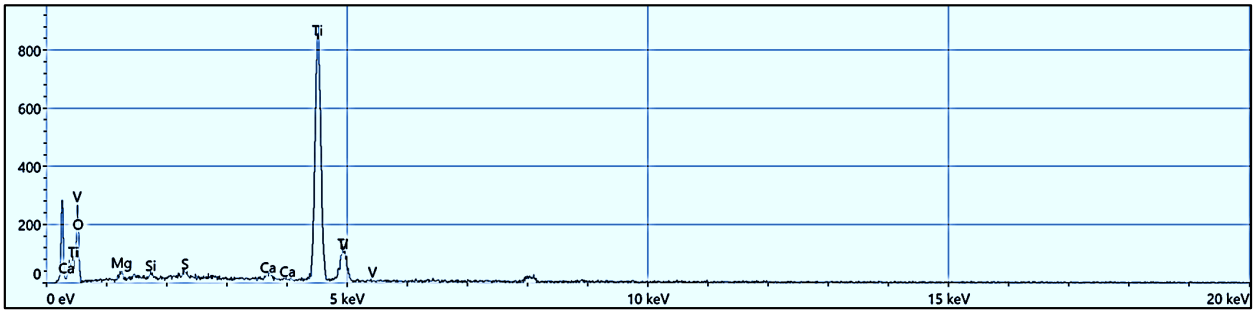

Figure 5. EDX spectrum of nano-TiO_2.

Table 7. EDX element results of NS.

Element	Atomic %	Atomic % Error	Weight %	Weight % Error
Si	29.9	0.1	42.7	0.1
O	69.7	0.4	56.6	0.3
Ca	0.0	0.0	0.7	0.0
Ci	0.3	0.0	0.1	0.0

Table 8. EDX element results of NT.

Element	Atomic %	Atomic % Error	Weight %	Weight % Error
Ti	18.2	0.1	39.4	0.2
O	79.2	1.3	57.1	0.9
Mg	1.2	0.1	1.3	0.1
Si	0.5	0.0	0.6	0.0
S	0.4	0.0	0.5	0.0
Ca	0.4	0.0	0.6	0.0
V	0.2	0.0	0.5	0.1

2.5. Nanomaterials Addition Method

A high-speed shear-mixer system (HSMS) was utilized to blend the nanomaterials with asphalt cement at specific speeds, temperatures, and durations to ensure that all the nanomaterials were distributed effectively. Table 9 presents the parameters of the nanomaterial addition method.

Table 9. Nanomaterial mixing conditions.

Nanoparticles	Temperature, °C	Time, min	Speed, rpm	Percent
NS	150 ± 5	60	3000	(2%, 4%, and 6%)
NT	155 ± 5	30	3500	(2%, 4%, and 6%)

3. Experimental Tests

3.1. Physical Binder Test

To ascertain the performance and consistency of the asphalt cement, a series of binder tests was conducted to assess the physical properties (with and without nanomaterials). The penetration test, in compliance with ASTM D5, provides insight into the binder's consistency through the use of a standard needle that penetrates the binder under specific conditions. The softening point test was performed following ASTM D36, indicating the flowability of asphalt at high temperatures. Additionally, the ductility test (ASTM D113) demonstrated the flexibility of the asphalt binder to elongate without breaking.

3.2. Marshall Test

The Marshall test was carried out following ASTM D6926. A batch weighing 1150 g and containing various percentages of aggregate and filler was mixed according to the aggregate gradation requirements. The aggregate blend was heated in a container for two hours at approximately 150 °C. Concurrently, the asphalt cement (4–6%) with an increment of 0.5 percent was heated at 155 °C for two hours to attain a viscosity of 170 cSt, as indicated in Figure 6. The materials were then mixed thoroughly for two minutes at 155 °C. The mixture was placed into cylindrical molds with a diameter of 100 mm and a height of 63 mm, and then heated for 10 min at 145 °C, corresponding to a viscosity of 280 cSt as per Figure 6. Specimens were compacted at both ends with 75 blows on each end using a Marshall hammer to simulate high-traffic conditions (>106 ESAL). The specimens' resistance to plastic flow was measured using the Marshall apparatus following ASTM D6927. The air content and void content in the mineral aggregate were also estimated based on the bulk-specific gravity (ASTM D2726) and the theoretical maximum specific gravity for each mixture (ASTM D2041).

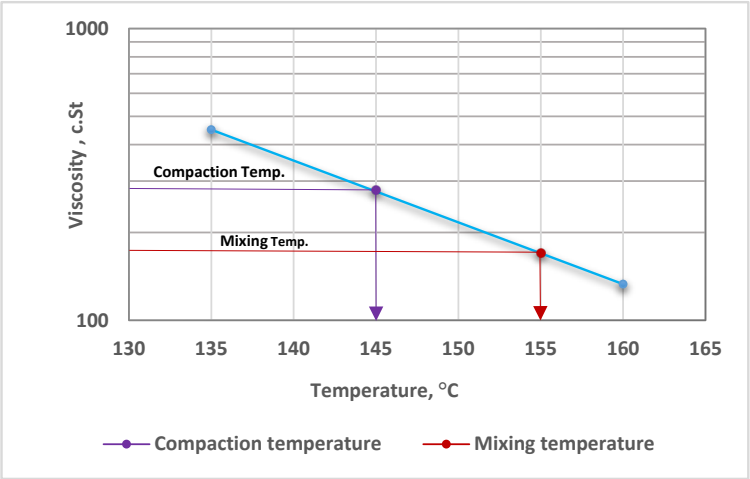

Figure 6. Viscosity–temperature relationship.

3.3. Indirect Tensile Strength Test

ASTM D4867 was used to assess the moisture susceptibility of the asphalt concrete mixtures. Specimens of each mix were prepared using the Marshall approach and compacted per face to reach 7 ± 1% air voids. Six specimens of each mix were prepared. They were then split into two groups: three control specimens tested at 25 °C, and three conditioned specimens exposed to a freezing and thawing cycle by conditioning at −18 ± 2 °C (16 h) and then 60 ± 1 °C (24 h), before conducting the tensile test at 25 °C. The compressive load in the indirect splitting tensile test was applied at a rate of 50.8 mm/min along the axis of the cylindrical specimens. These specimens failed by splitting along the vertical direction in the cross-sectional plane. The tensile strength was computed according to Equation (1). The tensile strength ratio (TSR), Equation (2), is the ratio of the tensile strength of the conditioned specimens (ITS_c) to that of the controls (ITS_d).

$$ITS = \frac{2000 \times Pmax}{\pi tD} \quad (1)$$

$$TSR = \frac{ITSc}{ITSd} \quad (2)$$

Here, ITS is the indirect tensile strength (kPa), Pmax is the maximum tensile load (N), D is the specimen diameter (mm), and t is the specimen thickness (mm). The TSR is the tensile strength ratio (%).

3.4. Compression Strength Test

The compression strength loss of the compacted asphalt concrete mixture specimens caused by water action was measured following ASTM D1075. Cylindrical specimens with dimensions of 100 mm × 100 mm were prepared following the procedure in ASTM D1074. The mixture was poured into the cylindrical mold in two layers and then subjected to an initial stress of 1 MPa, which was then increased to 20.7 MPa for two minutes to reach a specimen height of 100 mm. Six specimens were prepared of each mix. After that, they were split into two groups; the first group (dry specimens) was tested at 25 °C. The second group (wet specimens) was submerged in a water bath at 60 °C (24 h), then taken out and placed in another water bath at 25 °C (2 h), before testing by applying an axial load with a rate of 50.8 mm/min. The maximum compression load was recorded, and the compressive strength was obtained by dividing the load by the specimen cross-sectional area. The index of retained strength (IRS) was evaluated based on Equation (3):

$$IRS = \frac{CS_w}{CS_d} \times 100 \quad (3)$$

Here, CS_w is the wet compressive strength and CS_d is the dry compressive strength, both in units of kPa.

Table 10 summarizes the mixing ratios and tests covered in this study.

Table 10. Mixing ratios and tests.

Variables	Mixtures	Tests
Asphalt content	OAC − 0.5%	Modified binder tests: Penetration test (ASTM D5) Softening point test (ASTM D36) Ductility test (ASTM D113) Asphalt concrete tests: Tensile strength ratio test (ASTM D4867) Index of retained strength test (ASTM D1075)
	OAC	
	OAC + 0.5%	
Aggregate gradation (PNo. 4)	Mid-range −6%	
	Mid-range	
	Mid-range + 6%	
Hydrated lime at PNo. 4 levels	0% HL + PNo. 4 (mid-range −6%)	
	0% HL + PNo. 4 (mid-range)	
	0% HL + PNo. 4 (mid-range + 6%)	
	1.5% HL + PNo. 4 (mid-range −6%)	
	1.5% HL + PNo. 4 (mid-range)	
	1.5% HL + PNo. 4 (mid-range + 6%)	
Nano-silica	0% NS	
	2% NS	
	4% NS	
	6% NS	
Nano-titanium	0%NT	
	2% NT	
	4% NT	
	6% NT	

4. Results and Discussion

4.1. Impact of Nanomaterials on Asphalt Physical Properties

Both NS and NT affected the physical properties of the asphalt. The general trend indicated a reduction in the penetration value, an increase in the softening point, and a decrease in ductility. Figure 7a illustrates that as the NM content increased, the penetration value decreased. The reductions in the penetration value for NS at 2%, 4%, and 6% were 11.36%, 20.45%, and 34%, respectively, compared with the neat asphalt (0% NM). A similar pattern was observed for NT, with reductions of 6.81%, 13.63%, and 25%, respectively, at the same concentrations. NS displayed a more pronounced stiffening effect than NT, likely due to its higher specific surface area. Figure 7b shows that the addition of NS and NT to the asphalt positively affected the softening point. NS exhibited a greater increase than NT compared with neat asphalt, with increments of 3.84%, 9.61%, and 15.38% at 2%, 4%, and 6% NS, respectively, and 1.92%, 5.76%, and 11.53% at the same respective concentrations of NT. This trend suggested that both NS and NT enhanced asphalt's stiffness.

Figure 7c illustrates the ductility of asphalt with varying NM contents. Increasing NS and NT contents led to reductions in ductility by 7.97%, 14.49%, and 23.91% for NS and by 5.07%, 10.86%, and 17.39% for NT at 2%, 4%, and 6%, respectively. The decrease in ductility could be related to the reduced ability of the neat asphalt to elongate when NS and NT were dispersed within it. All results are consistent with findings reported in the literature [59–64].

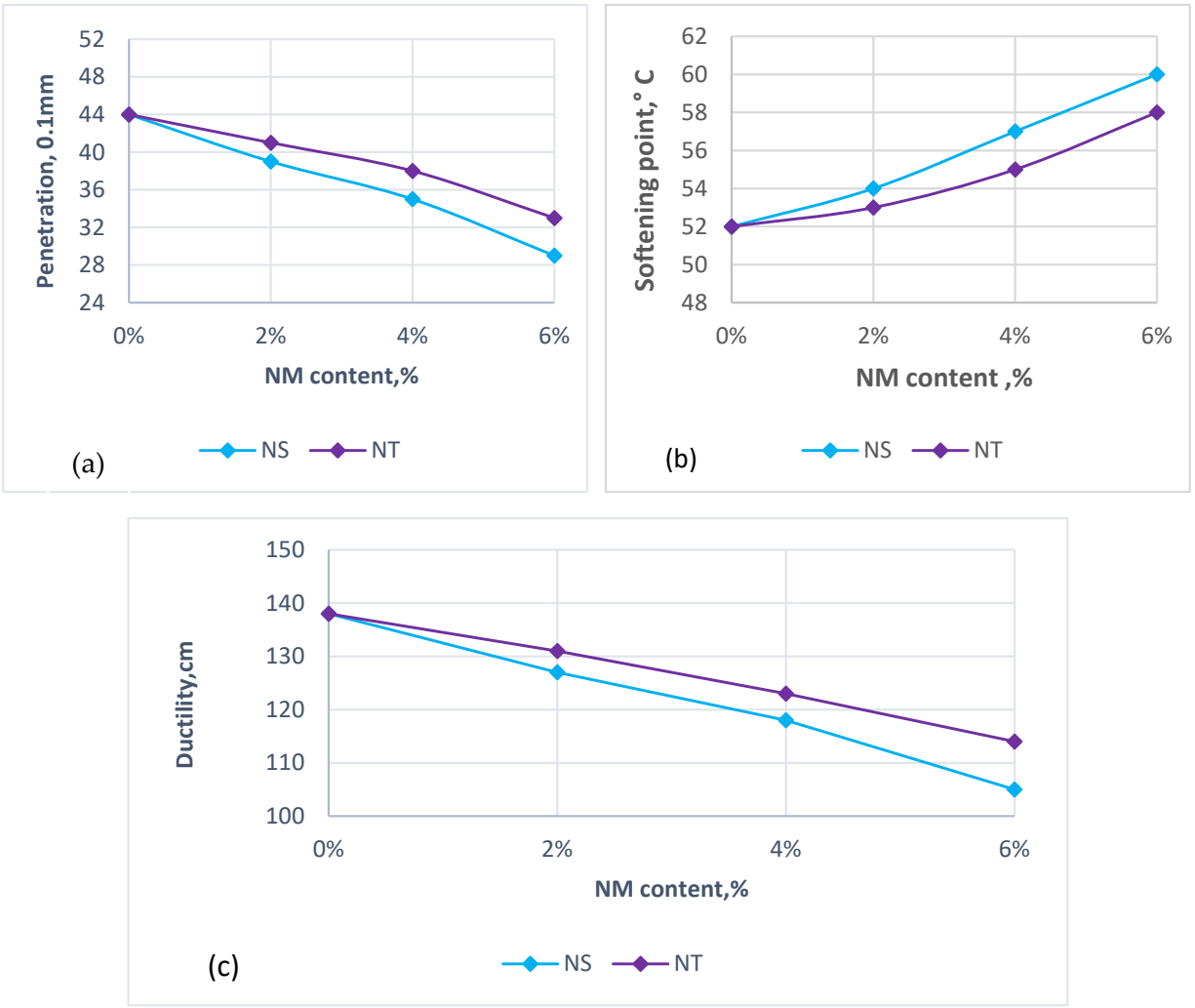

Figure 7. Effect of nanomaterials on physical characteristics of asphalt: (**a**) penetration, (**b**) softening point, and (**c**) ductility.

4.2. Marshall Test

The optimum asphalt content (OAC) for the asphalt mixture was computed using the Marshall mix design method. Five different asphalt concentrations were tested, ranging from 4% to 6% (by weight of the total mix) in increments of 0.5%. The OAC was determined by averaging the three asphalt contents that yielded maximum stability, maximum bulk density, and 4% air voids. Figure 8 displays the mix design results of the asphalt mixture. The OAC was found to be 4.9%. At this content, all the examined Marshall properties (voids in total mix, VTM; voids in mineral aggregates, VMA; and voids filled with asphalt, VFA) were within the specified limits [58]. The main aim of this study is to explore the effect of certain mix variables and modifiers on the mixture's ability to resist moisture damage. Therefore, the OAC of 4.9% determined for the control mix was maintained for all other types of mixtures rather than optimizing the mix design for each mixture type.

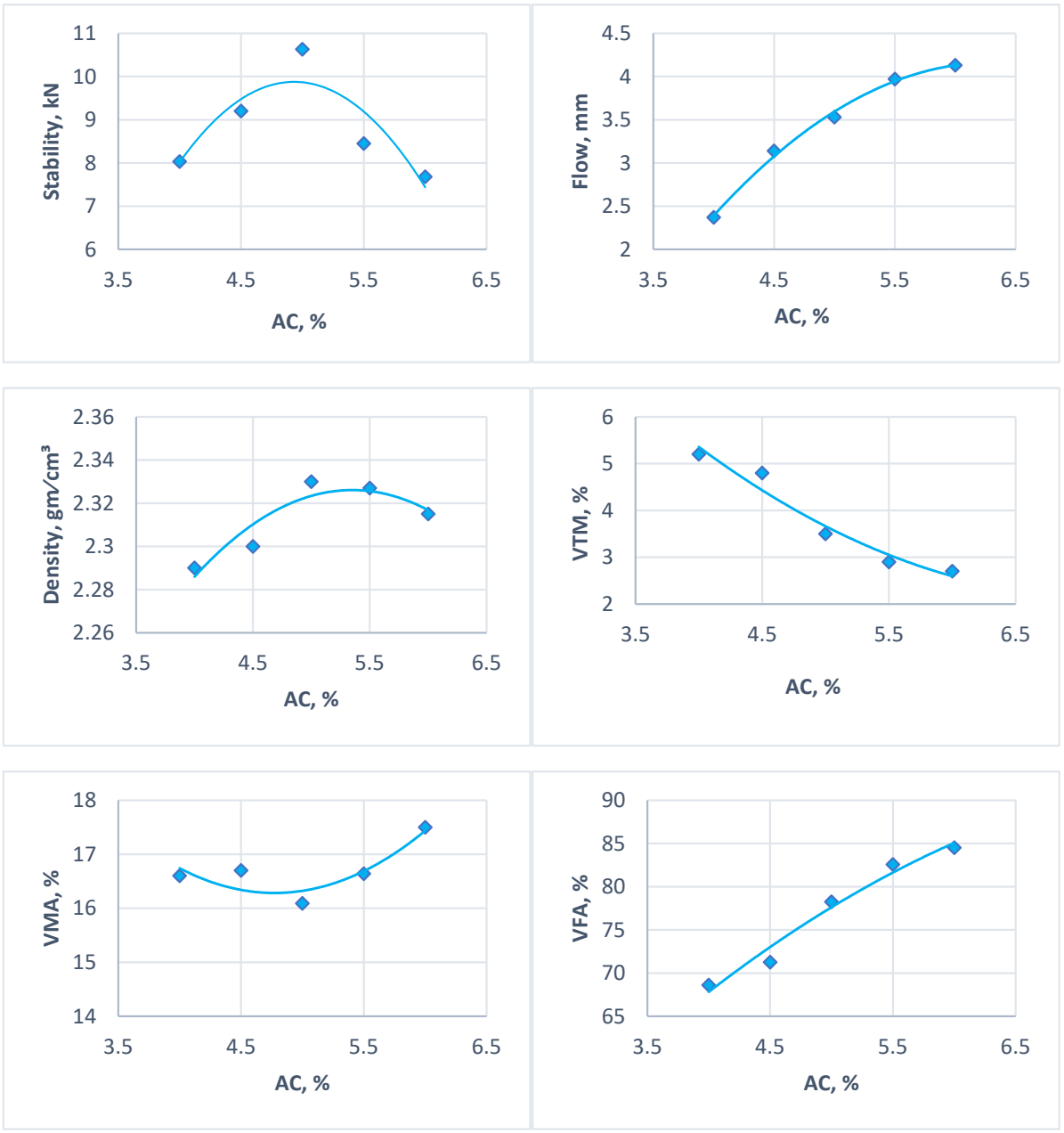

Figure 8. Marshall mix design results.

4.3. Indirect Tensile Strength Results

4.3.1. Effect of Mix Variables

Three asphalt contents of OAC, OAC − 0.5%, and OAC + 0.5% as well as three aggregate gradations with PNo. 4 equal to mid-range (59%), mid-range −6% (53%), and mid-range + 6% (65%) were used as mix variables in this study. Figure 9 illustrates the effect of AC on the tensile strength test. The mixture prepared with OAC (4.9%) had the highest tensile strength (both conditioned and unconditioned mixes). Consequently, the TSR also had the maximum value (80.45%) compared with mixtures prepared with other asphalt contents, meeting the minimum requirement of 80% specified in AASHTO T283. Insufficient AC led to impaired aggregate bonding. On the other hand, AC above the optimum level may lead to a thicker asphalt film around the aggregate and decrease the stiffness of the mixture because of the easy sliding of the aggregate particles against each other. The results are in agreement with those in [21,24].

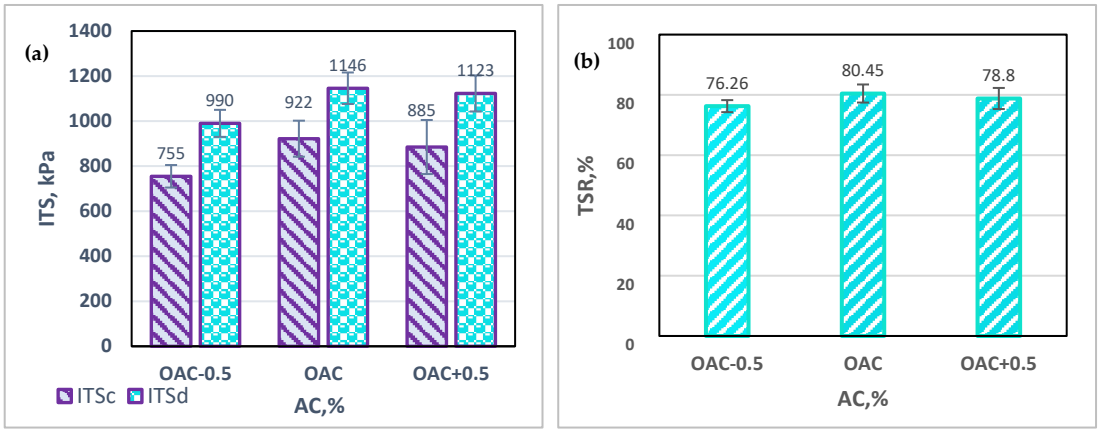

Figure 9. Effect of AC on (**a**) ITS and (**b**) TSR.

Figure 10 illustrates the impact of PNo. 4 on the tensile strength test. The ITS values improved when PNo. 4 increased, i.e., the fine aggregate fraction increased. The fine skeleton of aggregate with a high percentage of PNo. 4 resulted in a comparable increase in conditioned and unconditioned tensile strength. Furthermore, the TSR increased by 2.53% and 2.49% when PNo. 4 increased from 53 to 59 and from 59 to 65, respectively. The improved resistance to moisture damage with increasing PNo. 4 is likely due to better particle packing and reduced permeability, as the fine aggregate helps fill the voids between the coarse aggregate particles. This results in a denser structure that enhances the overall stability of the mixture. These outcomes are consistent with those obtained in [28,65].

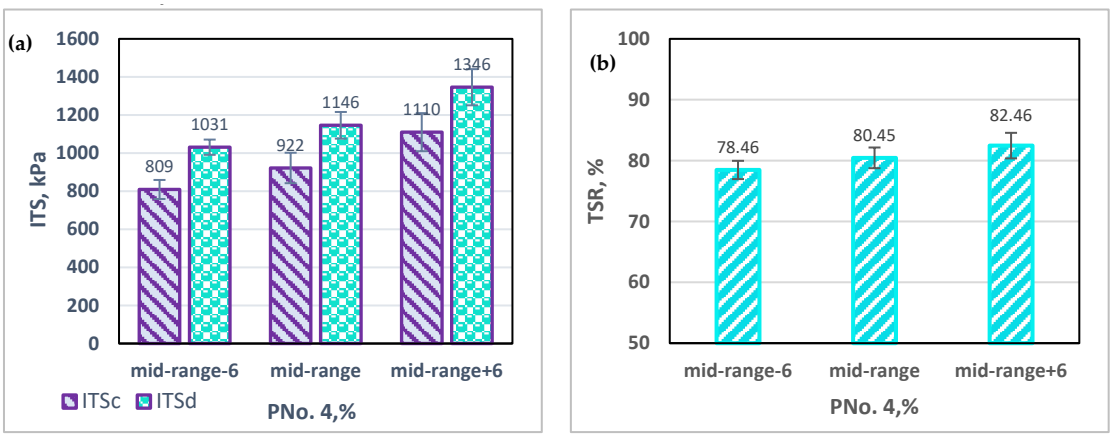

Figure 10. Effect of PNo. 4 on (**a**) ITS and (**b**) TSR.

4.3.2. Effect of Modifiers

Hydrated lime (HL) of a regular size, nano-silica oxide (NS), and nano-titanium dioxide (NT) were used as the modifiers in this study. Figure 11 shows the effect of HL on the tensile strength test at three different percentages of PNo. 4, indicating that the values of ITS and TSR improved in mixtures incorporating 1.5% HL as a partial replacement for LS. The TSR value increased by 2.93% at PNo. 4 (mid-range − 6%), 3.62% at PNo. 4 (mid-range), and 4.58% at PNo. 4 (mid-range + 6%) compared with the mixes containing only LS. Since HL particles have a high surface area, their ability to stiffen the asphalt matrix (asphalt cement and filler) is improved, leading to improved resistance to the tensile stress mobilized within a plane perpendicular to the diametral loading axis. Meanwhile, increasing PNo. 4 caused an additional improvement in tensile strength resistance against moisture damage, with the optimum value of TSR (86.24) at PNo. 4 (mid-range + 6%) + 1.5% HL. The results agreed with those in [29,33,66].

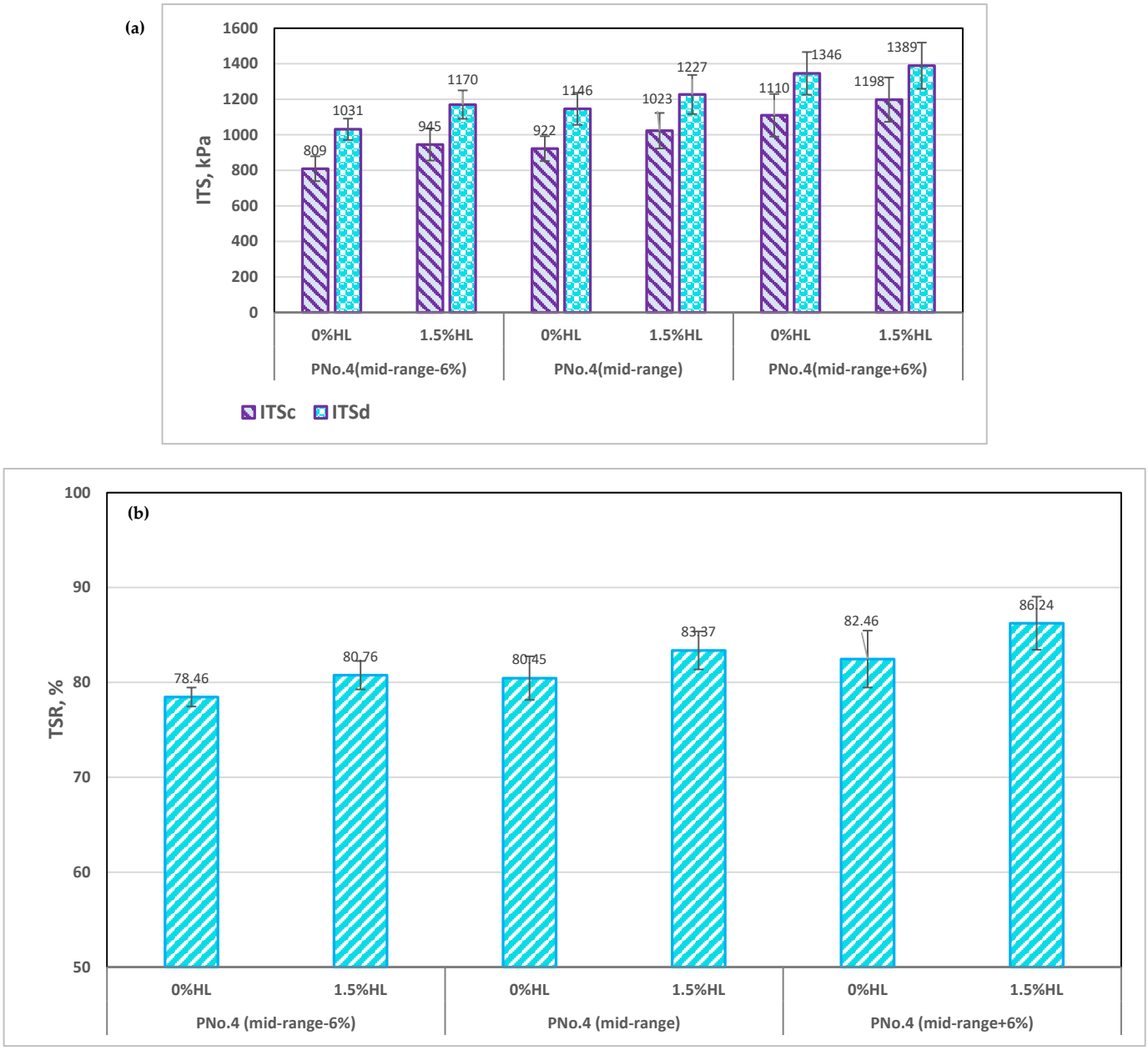

Figure 11. Effect of HL on (**a**) ITS and (**b**) TSR.

Based on the results displayed in Figure 12, the ITS of the mixtures modified with NS and NT was greater than that of the mixture without nanomaterials (0% NM). The ITS_d improvement percentages at 2%, 4%, and 6% NS were 20.15%, 24.17%, and 28.09%, respectively; the corresponding percentages for NT were 16.40%, 22.33%, and 26.96%. The ITS_c increased by 27.22%, 36.33%, and 46.96% for NS and by 21.25%, 32.75%, and 41.64% for NT at 2%, 4%, and 6%, respectively. Moreover, the optimum improvements in the TSR value for NS and NT were at 6% by 14.72% and 11.55%, respectively, compared with the mixture without nanomaterials (0% NM). The high specific surface area of NS, as shown in Table 6 (190~250 m^2/gm), allowed it to perform slightly better than NT in enhancing resistance to moisture damage. The extra fineness of NS leads to stronger adhesion between the aggregate particles and asphalt caused by increased asphalt cement stiffness, which minimizes the effect of stripping under the influence of moisture. This is similar to the findings of previous research [52,67–69].

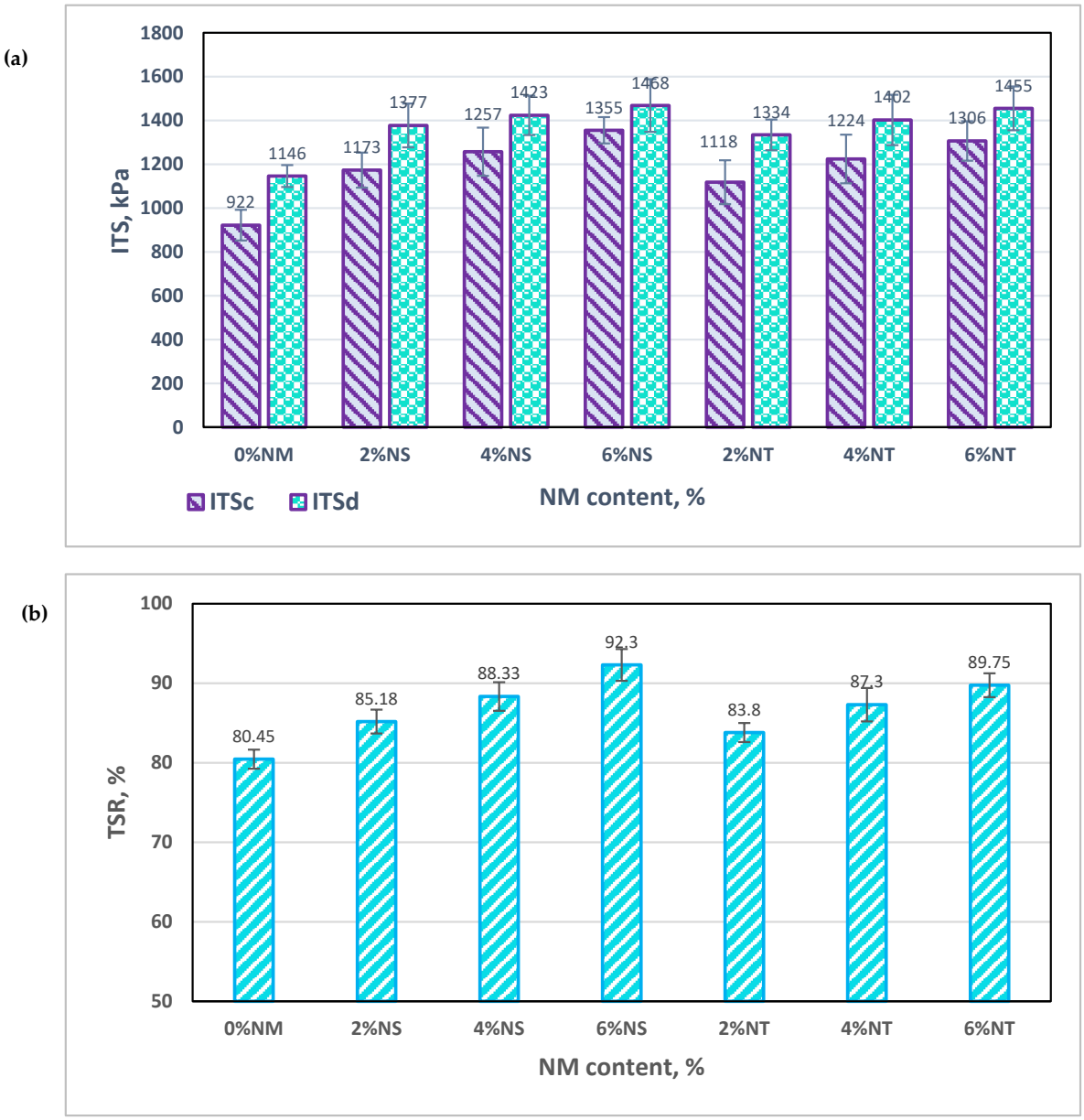

Figure 12. Effect of NMs on (**a**) ITS and (**b**) TSR.

4.3.3. Statistical Analysis

An analysis of variance (ANOVA) was conducted using Minitab software v17 to provide additional verification of the impact of the mix variables and modifiers on the moisture damage resistance of the asphalt concrete mixtures. *p*-values and *f*-values were employed to assess the significance of each factor, which is necessary for evaluating the significance of the variables and interpreting their reciprocal interactions. The outcomes of this analysis are based on the effect of the mix variables and modifiers on tensile strength, as reported in Table 11. The *p*-value falls below the significance level ($\alpha = 0.05$), and the *f*-value exceeds the *f*-critical value, which indicates that the outcomes are statistically significant. NS is the most significant factor due to its highest *f*-value, followed by NT, HL, PNo. 4, and AC.

Table 11. ANOVA results for the tensile strength test.

Source	DF	Adj SS	Adj MS	*f*-Value	*p*-Value	*f* Critical
PNo. 4	2	22.473	11.237	60.92	0.004	9.27
AC	2	12.544	6.272	34.00	0.009	
HL	1	14.920	14.920	80.89	0.003	
NS	3	116.644	38.881	210.79	0.001	
NT	3	75.925	25.308	137.21	0.001	
Error	3	0.553	0.184			
Lack-of-fit	2	0.553	0.276	*	*	
Pure error	1	0.000	0.0000			
Total	14	291.679				

4.4. Index of Retained Strength Test Results

4.4.1. Effect of Mix Variables

The variation in mix design variables in relation to the asphalt content and aggregate gradation can influence the compressive strength test. Figure 13 illustrates the effect of AC on the compression strength test. As the AC increased from OAC-0.5% to OAC, the CS_d and CS_w improved by 5.18% and 9.57%, respectively. When the AC was increased from OAC to OAC + 0.5%, it led to a slight drop in compressive strength in both dry and wet conditions, by 4.06% and 5.81%, respectively. This decline was due to softening of the asphalt mixture at AC above the optimum level. The results indicate that the mixture with OAC had the greatest value of IRS and that mixtures with variable asphalt content (OAC-0.5% and OAC + 0.5%) were unsusceptible to moisture since the IRS values were greater than 70%, as set by ASTM D1075.

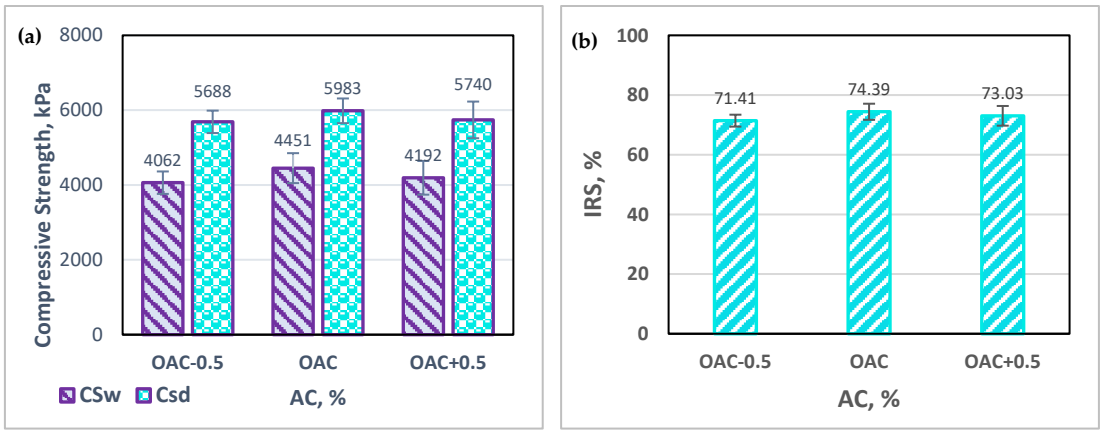

Figure 13. Effect of AC on (**a**) compressive strength and (**b**) IRS.

Figure 14 compares the effect of PNo. 4 on the compression strength test. When the rates of PNo. 4 increased, the CS_d and CS_w were enhanced. Therefore, the IRS increased by 2.59% and 3.69% when PNo. 4 increased from mid-range − 6% to mid-range and from mid-range to mid-range + 6%, respectively. The mixture prepared with a fine gradation (mid-range + 6%) had the highest moisture resistance owing to the fine particles' ability to fill the pores within the coarse aggregate skeleton, leading to enhanced adhesion between the asphalt cement and aggregate.

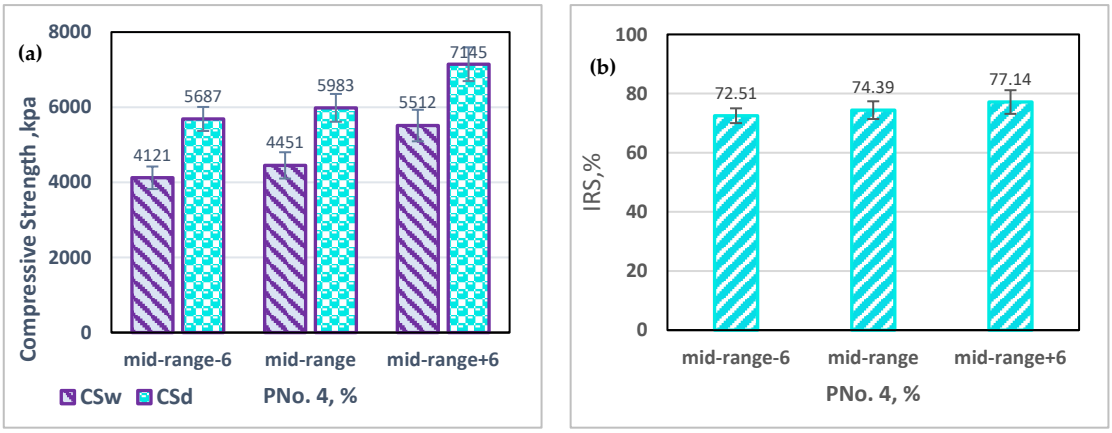

Figure 14. Effect of PNo. 4 on (**a**) compressive strength and (**b**) IRS.

4.4.2. Effect of Modifiers

To mitigate failure caused by moisture, it is desirable to use anti-stripping additives such as HL, NS, and NT. Figure 15 illustrates the effect of HL on the compression strength test. The outcomes revealed that using HL increased the dry and wet compressive strength more than did mixtures (0% HL) with different PNo. 4 levels. The C_w was lower than the C_d, which clarified the impact of moisture on mixes that exhibit moisture damage. The improvements in the IRS were 2.52 at PNo. 4 (mid-range − 6%), 4.20 at PNo. 4 (mid-range), and 3.96 at PNo. 4 (mid-range + 6%). The improved performance can be primarily attributed to the chemical reactions between HL and the asphalt binder and aggregate, wherein calcium ions (Ca++) in HL neutralize acidic components in the binder, improving adhesion and reducing moisture susceptibility. In addition, increasing the percentage of PNo. 4 led to better particle packing, which effectively resisted moisture damage. The results agreed with those in [66,70–73].

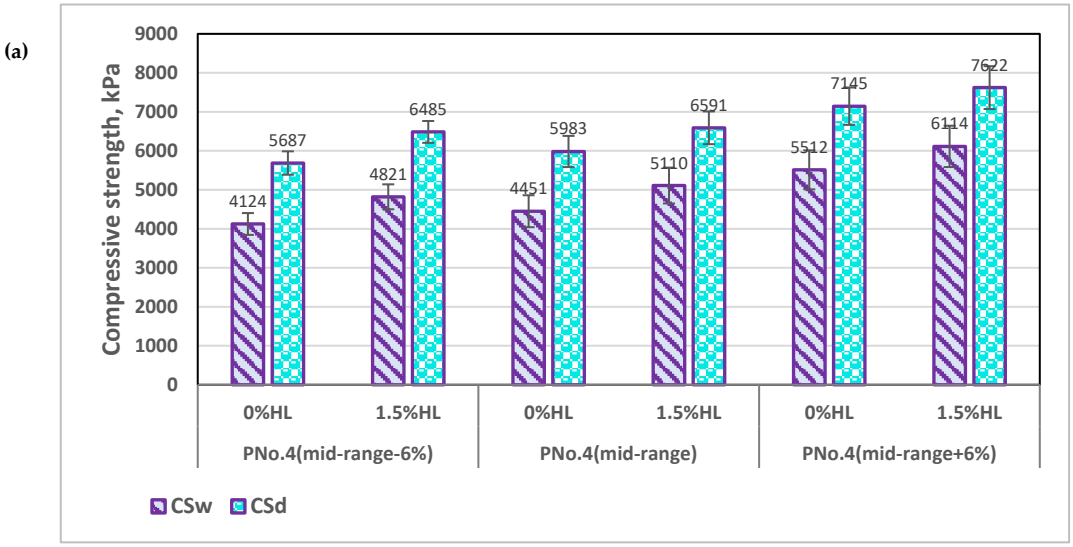

Figure 15. *Cont.*

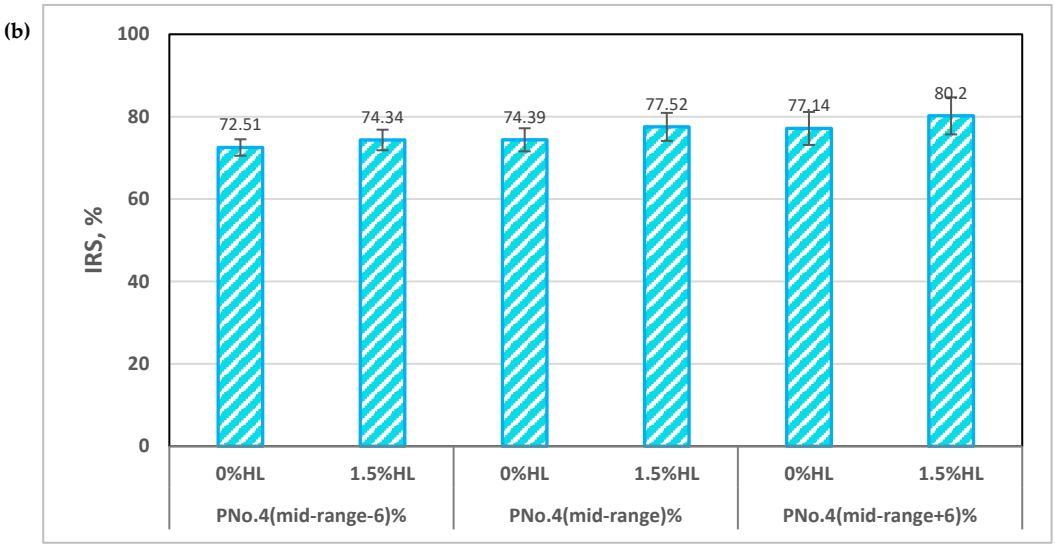

Figure 15. Effect of HL on (**a**) compressive strength and (**b**) IRS.

Figure 16 represents the relationship between the NMs (types and content) and the compression strength. The results indicate that incorporating NS and NT into the asphalt binder increased the values of both dry and wet compressive strength. This attribute led to a corresponding rise in the value of the IRS; the optimum increases in the IRS were obtained with 6% NS and NT, at 15.6% and 12.75%, respectively, relative to the 0% NM mixture. This improvement may be due to the physical properties and shape of these NMs, which had an essential effect on the interaction with the asphalt binder. Modifying the asphalt binder with NS and NT decreased the penetration grade shown in Figure 7, which led to stiffening the binder and enhancing the mixture's resistance against moisture damage.

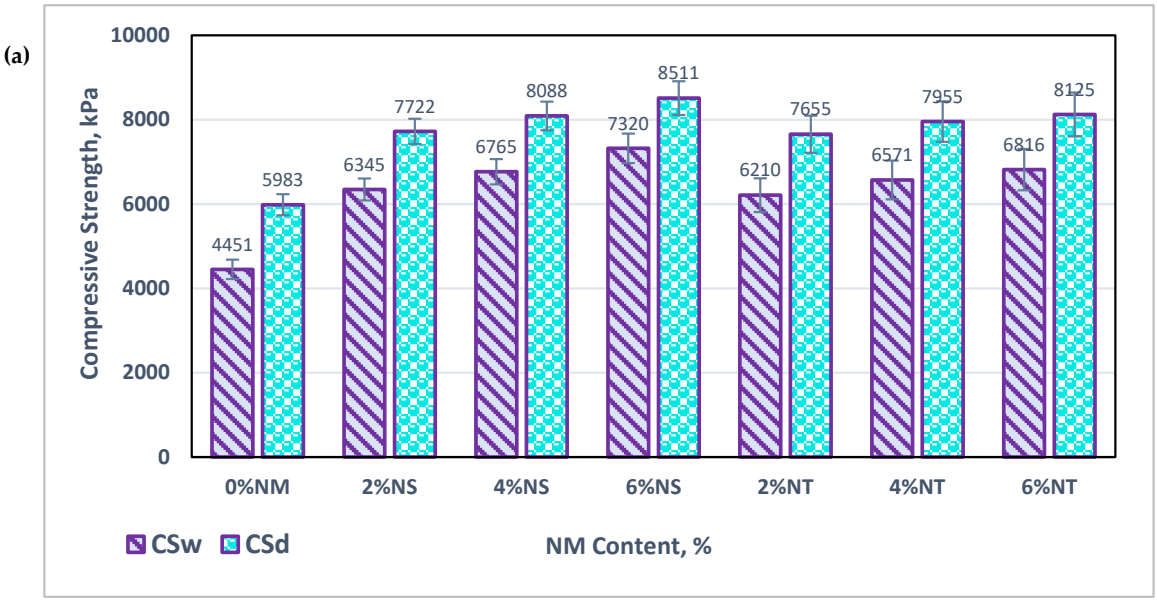

Figure 16. *Cont.*

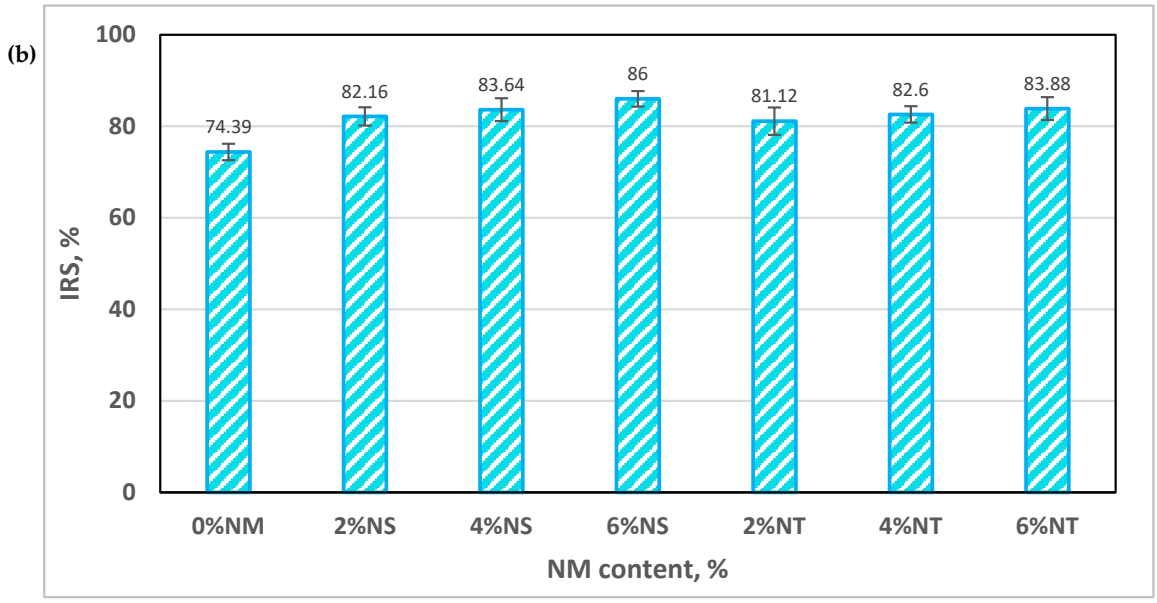

Figure 16. Effect of NMs on (**a**) compressive strength and (**b**) IRS.

4.4.3. Statistical Analysis

An analysis of variance (ANOVA) was conducted to identify the significant variables that influenced the compressive strength test. As shown in Table 12, the *f*-value demonstrated a statistically significant difference between the variables, which was higher than the *f*-critical for all cases, and the *p*-value was lower than the threshold for statistical significance ($\alpha = 0.05$). The ANOVA revealed the accurate significance of the variables, and the results indicated that the optimum significance was for NS, followed by NT, PNo. 4, HL, and AC.

Table 12. ANOVA results for the compressive strength test.

Source	DF	Adj SS	Adj MS	F-Value	*p*-Value	F-Critical
PNo. 4	2	27.553	13.777	73.03	0.003	9.27
AC	2	7.226	3.613	19.15	0.02	
HL	1	12.322	12.322	65.32	0.004	
NS	3	128.155	42.718	226.46	0.000	
NT	3	91.226	30.408	161.20	0.001	
Error	3	0.566	0.188			
Lack-of-fit	2	0.566	0.283	*	*	
Pure error	1	0.000	0.000			
Total	14	320.873				

Table 13 displays the optimal resistance against moisture damage based on the two types of tests used in this work to quantify the moisture damage resistance in relation to the mix variables and modifiers.

Table 13. The maximum moisture damage resistance in mixtures.

Mixture Type	TSR	IRS
Mix variables		
Mixture at OAC	80.45	74.39
PNo. 4 (mid-range + 6%)	82.46	77.14
Modifiers		
PNo. 4 (mid-range + 6%) + 1.5% HL	86.24	80.20
6% NS	92.30	86
6% NT	89.75	83.88

5. Conclusions

This study investigated the effects of mix design variables, such as the asphalt content and aggregate gradation (percent passing sieve No. 4), and modifiers, including hydrated lime (HL), nano-silica oxide (NS), and nano-titanium dioxide (NT), on the moisture damage resistance of asphalt concrete mixtures. Moisture damage was characterized using two types of indicators: the tensile strength ratio (TSR) and the index of retained strength (IRS). The following conclusions were drawn from the comprehensive laboratory experiments. While these findings provide valuable insights, further field studies are necessary to validate them and ensure their applicability in real-world pavement engineering practices.

1. Mix variables, particularly the asphalt content (AC) and aggregate gradation, significantly influenced moisture resistance. The optimal asphalt content (OAC) led to improved performance in TSR and IRS tests, with values of 80.45% and 74.39%, respectively. Fine gradation (mid-range + 6%) provided the best results for the TSR (82.46% at 0% HL and 86.24% at 1.5% HL) and IRS (77.14% at 0% HL and 80.20% at 1.5% HL) due to the dense structure and enhanced particle interlocking.
2. Substituting 1.5% HL for LS filler improved moisture resistance compared with mixtures without HL (0% HL), at each PNo. 4 level. The TSR increased by 2.93% at PNo. 4 (mid-range −6%), 3.62% at PNo. 4 (mid-range), and 4.58% at PNo. 4 (mid-range + 6%), while the IRS increased by 2.52%, 4.20%, and 3.96%, respectively.
3. The inclusion of nanomaterials (NS and NT) improved the physical properties of the asphalt binder by reducing penetration, raising the softening point, and decreasing ductility. SEM analysis showed that NS particles have a densely packed structure with a large surface area, which contributes to significant improvements in stiffness and resistance to moisture damage. NT particles, on the other hand, displayed spherical cluster shapes that facilitated homogeneous dispersion in the mixture.
4. NM additives significantly enhanced the mixture's performance against moisture susceptibility, as revealed by the TSR and IRS test results. A 6% dosage of NS and NT showed the best performance, with NS performing slightly better than NT. Optimal TSR values of 92.30 and 89.75 and IRS values of 86 and 83.88 were obtained with 6% NS and NT, respectively.
5. The ANOVA results provided valuable insights into the variables that had a significant impact on resisting moisture damage. In this study, both mix variables and modifiers were statistically significant with respect to the tensile strength and compression strength tests. It was observed that NS had the highest level of significance, while AC had the lowest significance compared with other variables.

Overall, this study's findings clearly demonstrate that proper mix design along with modifiers, particularly nanomaterials and hydrated lime, significantly affects moisture damage in asphalt concrete mixtures. However, these findings are based on systematic laboratory work; practical engineering application is crucial for promoting the actual performance of asphalt pavements.

Author Contributions: Conceptualization, N.N.A. and A.H.A.; methodology, A.H.A.; software, A.H.A.; validation, N.N.A.; formal analysis, A.H.A.; investigation, A.H.A.; resources, A.H.A.; data curation, N.N.A.; writing—original draft preparation, N.N.A.; writing—review and editing, A.H.A.; visualization, A.H.A.; supervision, A.H.A.; project administration, A.H.A.; funding acquisition, N.N.A. All authors have read and agreed to the published version of the manuscript.

Funding: This research received no external funding.

Data Availability Statement: Data will be made available on request.

Conflicts of Interest: The authors declare that there are no conflicts of interest regarding the publication of this paper.

References

1. Styer, J.; Tunstall, L.; Landis, A.; Grenfell, J. Innovations in Pavement Design and Engineering: A 2023 Sustainability Review. *Heliyon* **2024**, *10*, e33602. [CrossRef] [PubMed]
2. Omar, H.A.; Yusoff, N.I.M.; Mubaraki, M.; Ceylan, H. Effects of Moisture Damage on Asphalt Mixtures. *J. Traffic Transp. Eng.* **2020**, *7*, 600–628. [CrossRef]
3. Kringos, N.; Scarpas, A. Physical and Mechanical Moisture Susceptibility of Asphaltic Mixtures. *Int. J. Solids Struct.* **2008**, *45*, 2671–2685. [CrossRef]
4. Raza, A.; Khan, I.; Tufail, R.F.; Frankovska, J.; Mushtaq, M.U.; Salmi, A.; Awad, Y.A.; Javed, M.F. Evaluation of Moisture Damage Potential in Hot Mix Asphalt Using Polymeric Aggregate Treatment. *Materials* **2022**, *15*, 5437. [CrossRef] [PubMed]
5. Liu, S.; Zhou, S.; Peng, A. Analysis of Moisture Susceptibility of Foamed Warm Mix Asphalt Based on Cohesion, Adhesion, Bond Strength, and Morphology. *J. Clean. Prod.* **2020**, *277*, 123334. [CrossRef]
6. Zhu, J.; Zhang, K.; Liu, K.; Shi, X. Adhesion Characteristics of Graphene Oxide Modified Asphalt Unveiled by Surface Free Energy and AFM-Scanned Micro-Morphology. *Constr. Build. Mater.* **2020**, *244*, 118404. [CrossRef]
7. Liu, X.; Sha, A.; Li, C.; Zhang, Z.; Li, H. Influence of Water on Warm-Modified Asphalt: Views from Adhesion, Morphology and Chemical Characteristics. *Constr. Build. Mater.* **2020**, *264*, 120159. [CrossRef]
8. Notani, M.A.; Hajikarimi, P.; Moghadas Nejad, F.; Khodaii, A. Performance Evaluation of Using Waste Toner in Bituminous Material by Focusing on Aging and Moisture Susceptibility. *J. Mater. Civ. Eng.* **2021**, *33*, 04020405. [CrossRef]
9. Zhou, L.; Huang, W.; Zhang, Y.; Lv, Q.; Yan, C.; Jiao, Y. Evaluation of the Adhesion and Healing Properties of Modified Asphalt Binders. *Constr. Build. Mater.* **2020**, *251*, 119026. [CrossRef]
10. Sengoz, B.; Agar, E. Effect of Asphalt Film Thickness on the Moisture Sensitivity Characteristics of Hot-Mix Asphalt. *Build. Environ.* **2007**, *42*, 3621–3628. [CrossRef]
11. Hasan, E.A.; Abed, Y.H.; Abedali Al-Haddad, A.H. Improved Adhesion Bond between Asphalt Binder-Aggregate as Indicator to Reduced Moisture Damage. *J. Phys. Conf. Ser.* **2021**, *1973*, 012059. [CrossRef]
12. XIONG Rui GUAN Bowen, C.S. Application of Grey Entropy Method to Analyze Influencing Factors of Durability of Asphalt Mixture under Freeze-Thaw and Corrosion. *J. Highw. Transp. Res. Dev.* **2013**, *30*, 28–32.
13. Xiong, R.; Chu, C.; Qiao, N.; Wang, L.; Yang, F.; Sheng, Y.; Guan, B.; Niu, D.; Geng, J.; Chen, H. Performance Evaluation of Asphalt Mixture Exposed to Dynamic Water and Chlorine Salt Erosion. *Constr. Build. Mater.* **2019**, *201*, 121–126. [CrossRef]
14. Ma, Y.; Elseifi, M.A.; Dhakal, N.; Bashar, M.Z.; Zhang, Z. Non-Destructive Detection of Asphalt Concrete Stripping Damage Using Ground Penetrating Radar. *Transp. Res. Rec.* **2021**, *2675*, 938–947. [CrossRef]
15. Lucas Júnior, J.L.O.; Babadopulos, L.F.A.L.; Soares, J.B.; Souza, L.T. Evaluating the Effect of Amine-Based Anti-Stripping Agent on the Fatigue Life of Asphalt Pavements. *Int. J. Pavement Eng.* **2022**, *23*, 2785–2795. [CrossRef]
16. Xiao, R.; Ding, Y.; Polaczyk, P.; Ma, Y.; Jiang, X.; Huang, B. Moisture Damage Mechanism and Material Selection of HMA with Amine Antistripping Agent. *Mater. Des.* **2022**, *220*, 110797. [CrossRef]
17. Yang, S.L.; Baek, C.; Park, H.B. Effect of Aging and Moisture Damage on Fatigue Cracking Properties in Asphalt Mixtures. *Appl. Sci.* **2021**, *11*, 10543. [CrossRef]
18. Ali, Y.; Irfan, M.; Buller, A.S.; Khan, H.A.; Gul, H.M.F. A Binary Logistic Model for Predicting the Tertiary Stage of Permanent Deformation of Conventional Asphalt Concrete Mixtures. *Constr. Build. Mater.* **2019**, *227*, 116608. [CrossRef]
19. Anastasio, S.; Perez Fortes, A.P.; Hoff, I. Effect of Aggregate Petrology on the Durability of Asphalt Pavements. *Constr. Build. Mater.* **2017**, *146*, 652–657. [CrossRef]
20. Othman, M.; Rafiq, M.; Rosli, M. Jurnal Teknologi An Overview of Moisture Damage in Asphalt Mixtures. *J. Teknol.-UTM* **2015**, *4*, 125–131.
21. Sarsam, S.I.; Alwan, A.H. Impact of Moisture Damage on Rutting Resistance, Shear and Tensile Properties of Asphalt Pavement. *Int. J. Sci. Res. Knowl.* **2014**, *2*, 453–462. [CrossRef]
22. Abu Abdo, A.M.; Jung, S.J. Effects of Asphalt Mix Design Properties on Pavement Performance: A Mechanistic Approach. *Adv. Civ. Eng.* **2016**, *2016*, 04020405. [CrossRef]

23. Zeiada, W.; Abu Dabous, S.; Al-Ruzouq, R.; Hamad, K.; Souliman, M.; Mirou, S. Effect of Air Voids and Asphalt Content Changes on Laboratory and Simulated Long-Term Fatigue Performance of Asphalt Concrete Pavements. *Innov. Infrastruct. Solut.* **2022**, *8*, 48. [CrossRef]
24. Ziari, H.; Hajiloo, M. The Effect of Mix Design Method on Performance of Asphalt Mixtures Containing Reclaimed Asphalt Pavement and Recycling Agents: Superpave versus Balanced Mix Design. *Case Stud. Constr. Mater.* **2023**, *18*, e01931. [CrossRef]
25. Kanitpong, K.; Charoentham, N.; Likitlersuang, S. Investigation on the Effects of Gradation and Aggregate Type to Moisture Damage of Warm Mix Asphalt Modified with Sasobit. *Int. J. Pavement Eng.* **2012**, *13*, 451–458. [CrossRef]
26. Aodah, H.; Chandra, S.; Kareem, Y.A. Estimation of Moisture Damage and Permanent Deformation in Asphalt Mixture from Aggregate Gradation. *KSCE J. Civ. Eng.* **2014**, *18*, 1655–1663.
27. Sangsefidi, E.; Ziari, H.; Sangsefidi, M. The Effect of Aggregate Gradation Limits Consideration on Performance Properties and Mixture Design Parameters of Hot Mix Asphalt. *KSCE J. Civ. Eng.* **2015**, *20*, 385–392. [CrossRef]
28. Ezzat, E.N.; Abed, A.H. The Influence of Using Hybrid Polymers, Aggregate Gradation and Fillers on Moisture Sensitivity of Asphaltic Mixtures. *Mater. Today Proc.* **2020**, *20*, 493–498. [CrossRef]
29. Lesueur, D.; Petit, J.; Ritter, H.J. The Mechanisms of Hydrated Lime Modification of Asphalt Mixtures: A State-of-the-Art Review. *Road Mater. Pavement Des.* **2013**, *14*, 1–16. [CrossRef]
30. Preti, F.; Accardo, C.; Gouveia, B.C.S.; Romeo, E.; Tebaldi, G. Influence of High-Surface-Area Hydrated Lime on Cracking Performance of Open-Graded Asphalt Mixtures. *Road Mater. Pavement Des.* **2021**, *22*, 2654–2660. [CrossRef]
31. Al-Bayati, H.K.A.; Oyeyi, A.G.; Tighe, S.L. Experimental Assessment of Mineral Filler on the Volumetric Properties and Mechanical Performance of Hma Mixtures. *Civ. Eng. J.* **2020**, *6*, 2312–2331. [CrossRef]
32. Grajales, J.A.; Pérez, L.M.; Schwab, A.P.; Little, D.N. Quantum Chemical Modeling of the Effects of Hydrated Lime (Calcium Hydroxide) as a Filler in Bituminous Materials. *ACS Omega* **2021**, *6*, 3130–3139. [CrossRef] [PubMed]
33. Albayati, A.; Wang, Y.; Haynes, J. Size Effect of Hydrated Lime on the Mechanical Performance of Asphalt Concrete. *Materials* **2022**, *15*, 3715. [CrossRef] [PubMed]
34. Alabady, H.; Abed, A. Effect of Quality and Quantity of Locally Produced Filler on Moisture Damage Hot Asphaltic Mixtures. *E3S Web Conf.* **2023**, *427*, 3039. [CrossRef]
35. Liang, Y.; Bai, T.; Zhou, X.; Wu, F.; Chenxin, C.; Peng, C.; Fuentes, L.; Walubita, L.F.; Li, W.; Wang, X. Assessing the Effects of Different Fillers and Moisture on Asphalt Mixtures' Mechanical Properties and Performance. *Coatings* **2023**, *13*, 288. [CrossRef]
36. Behiry, A.E.A.E.M. Laboratory Evaluation of Resistance to Moisture Damage in Asphalt Mixtures. *Ain Shams Eng. J.* **2013**, *4*, 351–363. [CrossRef]
37. Zghair, H.; Joni, H.; Hassan, M. Influence of Micro- Size Silica Powder on Physical and Rheological Characteristics of Asphalt Binder. *Int. J. Eng. Technol.* **2018**, *7*, 180. [CrossRef]
38. Tanzadeh, R.; Shafabakhsh, G. Surface Free Energy and Adhesion Energy Evaluation of Modified Bitumen with Recycled Carbon Black (Micro-Nano) from Gases and Petrochemical Waste. *Constr. Build. Mater.* **2020**, *245*, 118361. [CrossRef]
39. Aljbouri, H.J.; Albayati, A.H. Effect of Nanomaterials on the Durability of Hot Mix Asphalt. *Transp. Eng.* **2023**, *11*, 100165. [CrossRef]
40. Diab, A.; You, Z.; Hossain, Z.; Zaman, M. Moisture Susceptibility Evaluation of Nanosize Hydrated Lime-Modified Asphalt-Aggregate Systems Based on Surface Free Energy Concept. *Transp. Res. Rec.* **2024**, *2446*, 52–59. [CrossRef]
41. Wang, Y.; Latief, R.H.; Al-mosawe, H.; Mohammad, H.K.; Albayati, A.; Haynes, J. Influence of Iron Filing Waste on the Performance of Warm Mix Asphalt. *Sustainability* **2021**, *13*, 13828. [CrossRef]
42. Lima, O.; Afonso, C.; Segundo, I.R.; Landi, S.; Homem, N.C.; Freitas, E.; Alcantara, A.; Branco, V.C.; Soares, S.; Soares, J.; et al. Asphalt Binder "Skincare"? Aging Evaluation of an Asphalt Binder Modified by Nano-TiO_2. *Nanomaterials* **2022**, *12*, 1678. [CrossRef] [PubMed]
43. Aljbouri, R.Q.; Albayati, A.H. Investigating the Effect of Nanomaterials on the Marshall Properties and Durability of Warm Mix Asphalt. *Cogent Eng.* **2023**, *10*, 2269640. [CrossRef]
44. Li, J.; Tang, F. Effects of Two Metal Nanoparticles on Performance Properties of Asphalt Binder and Stone Matrix Asphalt Mixtures Containing Waste High Density Polyethelene. *Constr. Build. Mater.* **2023**, *401*, 132787. [CrossRef]
45. Yusoff, N.I.M.; Breem, A.A.S.; Alattug, H.N.M.; Hamim, A.; Ahmad, J. The Effects of Moisture Susceptibility and Ageing Conditions on Nano-Silica/Polymer-Modified Asphalt Mixtures. *Constr. Build. Mater.* **2014**, *72*, 139–147. [CrossRef]
46. Fusco, R.; Moretti, L.; Fiore, N.; D'andrea, A. Behavior Evaluation of Bituminous Mixtures Reinforced with Nano-Sized Additives: A Review. *Sustainability* **2020**, *12*, 8044. [CrossRef]
47. Bala, N.; Napiah, M.; Kamaruddin, I. Nanosilica Composite Asphalt Mixtures Performance-Based Design and Optimisation Using Response Surface Methodology. *Int. J. Pavement Eng.* **2018**, *8436*, 29–40. [CrossRef]
48. Yang, S.; Yan, K.; Liu, W. The Effect of Ultraviolet Aging Duration on the Rheological Properties of Sasobit/SBS/Nano-TiO_2-Modified Asphalt Binder. *Appl. Sci.* **2022**, *12*, 10600. [CrossRef]
49. Alhamali, D.; Wu, J.; Liu, Q.; Hassan, N.; Md Yusoff, N.I.; Ali, S. Physical and Rheological Characteristics of Polymer Modified Bitumen with Nanosilica Particles. *Arab. J. Sci. Eng.* **2015**, *41*, 946–961. [CrossRef]
50. Azarhoosh, A.; Moghaddas Nejad, F.; Khodaii, A. Evaluation of the Effect of Nano-TiO_2 on the Adhesion between Aggregate and Asphalt Binder in Hot Mix Asphalt. *Eur. J. Environ. Civ. Eng.* **2018**, *22*, 946–961. [CrossRef]

51. Saltan, M.; Terzi, S.; Karahancer, S. Examination of Hot Mix Asphalt and Binder Performance Modified with Nano Silica. *Constr. Build. Mater.* **2017**, *156*, 976–984. [CrossRef]
52. Buhari, R.; Abdullah, M.E.; Ahmad, M.K.; Zabidi, N.; Bakar, S.K.A. Moisture Susceptibility of Modified Asphalt Concrete Containing Titanium Dioxide. *Int. J. Adv. Trends Comput. Sci. Eng.* **2019**, *8*, 140–143. [CrossRef]
53. Sezavar, R.; Shafabakhsh, G.; Mirabdolazimi, S.M. New Model of Moisture Susceptibility of Nano Silica-Modified Asphalt Concrete Using GMDH Algorithm. *Constr. Build. Mater.* **2019**, *211*, 528–538. [CrossRef]
54. Mirabdolazimi, S.M.; Kargari, A.H.; Pakenari, M.M. New Achievement in Moisture Sensitivity of Nano-Silica Modified Asphalt Mixture with a Combined Effect of Bitumen Type and Traffic Condition. *Int. J. Pavement Res. Technol.* **2021**, *14*, 105–115. [CrossRef]
55. Dell'Antonio Cadorin, N.; Victor Staub de Melo, J.; Borba Broering, W.; Luiz Manfro, A.; Salgado Barra, B. Asphalt Nanocomposite with Titanium Dioxide: Mechanical, Rheological and Photoactivity Performance. *Constr. Build. Mater.* **2021**, *289*, 18–25. [CrossRef]
56. Masri, K.; Zali, N.; Putra Jaya, R.; Abu Seman, M.; Mohd Hasan, M.R. The Influence of Nano Titanium as Bitumen Modifier in Stone Mastic Asphalt. *Adv. Mater. Sci. Eng.* **2022**, *2022*, 4021618. [CrossRef]
57. Mohammed, A.M.; Abed, A.H. Effect of Nano-TiO2 on Physical and Rheological Properties of Asphalt Cement. *Open Eng.* **2024**, *14*, 20220520. [CrossRef]
58. *SCRB/R9*; Standard Specifications for Roads and Bridges, Section R/9, Hot-Mix Asphaltic Concrete Pavement. Revised Edition. State Corporation of Roads and Bridges, Ministry of Housing and Construction: Baghdad, Iraq, 2003.
59. Shafabakhsh, G.; Mirabdolazimi, S.M.; Sadeghnejad, M. Evaluation the Effect of Nano-TiO_2 on the Rutting and Fatigue Behavior of Asphalt Mixtures. *Constr. Build. Mater.* **2014**, *54*, 566–571. [CrossRef]
60. Enieb, M.; Diab, A. Characteristics of Asphalt Binder and Mixture Containing Nanosilica. *Int. J. Pavement Res. Technol.* **2017**, *10*, 148–157. [CrossRef]
61. Taherkhani, H.; Tajdini, M. Comparing the Effects of Nano-Silica and Hydrated Lime on the Properties of Asphalt Concrete. *Constr. Build. Mater.* **2019**, *218*, 308–315. [CrossRef]
62. Al-Sabaeei, A.M.; Napiah, M.B.; Sutanto, M.H.; Alaloul, W.S.; Zoorob, S.E.; Usman, A. Influence of Nanosilica Particles on the High-Temperature Performance of Waste Denim Fibre-Modified Bitumen. *Int. J. Pavement Eng.* **2022**, *23*, 207–220. [CrossRef]
63. Mohammed, A.M.; Abed, A.H. Enhancing Asphalt Binder Performance through Nano-SiO_2 and Nano-$CaCO_3$ Additives: Rheological and Physical Insights. *Case Stud. Constr. Mater.* **2023**, *19*, e02492. [CrossRef]
64. Albayati, A.H.; Latief, R.H.; Al-Mosawe, H.; Wang, Y. Nano-Additives in Asphalt Binder: Bridging the Gap between Traditional Materials and Modern Requirements. *Appl. Sci.* **2024**, *14*, 3998. [CrossRef]
65. Abo-Qudais, S.; Al-Shweily, H. Effect of Aggregate Properties on Asphalt Mixtures Stripping and Creep Behavior. *Constr. Build. Mater.* **2007**, *21*, 1886–1898. [CrossRef]
66. Ali, S.; Ismael, M. Improving the Moisture Damage Resistance of HMA by Using Ceramic Fiber and Hydrated Lime. *Al-Qadisiyah J. Eng. Sci.* **2020**, *13*, 274–283.
67. Rasheed, S.S.; Joni, H.H.; Al-Rubaee, R.H. Using Nano Silica to Improve Asphalt Mixture Performance. *AIP Conf. Proc.* **2023**, *2775*, 060005.
68. Razavi, S.H.; Kavussi, A. The Role of Nanomaterials in Reducing Moisture Damage of Asphalt Mixes. *Constr. Build. Mater.* **2020**, *239*, 117827. [CrossRef]
69. Taher, Z.K.; Ismael, M.Q. Moisture Susceptibility of Hot Mix Asphalt Mixtures Modified by Nano Silica and Subjected to Aging Process. *J. Eng.* **2023**, *29*, 128–143. [CrossRef]
70. Ahmed, A.H.; Ismael, M.Q. Effect of Hydrated Lime on Moisture Susceptibility of Asphalt Mixtures. *J. Eng.* **2019**, *25*, 89–101.
71. Abd Al Kareem, H.M.; Albayati, A.H. The possibility of minimizing rutting distress in asphalt concrete wearing course. *Eng. Technol. Appl. Sci. Res.* **2022**, *12*, 8063–8074. [CrossRef]
72. Albayati, A.H.; Al-Mosawe, H.M.; Allawi, A.A.; Oukaili, N. Moisture susceptibility of sustainable warm mix asphalt. *Adv. Civ. Eng.* **2018**, *2018*, 3109435. [CrossRef]
73. Albayati, A.; Al-Mosawe, H.; Sukhija, M.; Naidu, A.N. Appraising the synergistic use of recycled asphalt pavement and recycled concrete aggregate for the production of sustainable asphalt concrete. *Case Stud. Constr. Mater.* **2023**, *19*, e02237. [CrossRef]